Published in final edited form as:
Insect Biochem Mol Biol. 2014 July ; 50: 82–91. doi:10.1016/j.ibmb.2014.04.005.

Manduca sexta prophenoloxidase activating proteinase-3 (PAP3) stimulates melanization by activating proPAP3, proSPHs, and proPOs

Yang Wang, **Zhiqiang Lu**, and **Haobo Jiang**
Department of Entomology and Plant Pathology, Oklahoma State University, Stillwater, OK 74078

Abstract

Melanization participates in various insect physiological processes including antimicrobial immune responses. Phenoloxidase (PO), a critical component of the enzyme system catalyzing melanin formation, is produced as an inactive precursor prophenoloxidase (proPO) and becomes active via specific proteolytic cleavage by proPO activating proteinase (PAP). In *Manduca sexta*, three PAPs can activate proPOs in the presence of two serine proteinase homologs (SPH1 and SPH2). While the hemolymph proteinases (HPs) that generate the active PAPs are known, it is unclear how the proSPHs (especially proSPH1) are activated. In this study, we isolated from plasma of bar-stage *M. sexta* larvae an Ile-Glu-Ala-Arg-*p*-nitroanilide hydrolyzing enzyme that cleaved the proSPHs. This proteinase, PAP3, generated active SPH1 and SPH2, which function as cofactors for PAP3 in proPO activation. Cleavage of the purified recombinant proSPHs by PAP3 yielded 38 kDa bands similar in mobility to the SPHs formed *in vivo*. Surprisingly, PAP3 also can activate proPAP3 to stimulate melanization in a direct positive feedback loop. The enhanced proPO activation concurred with the cleavage activation of proHP6, proHP8, proPAP1, proPAP3, proSPH1, proSPH2, proPOs, but not proHP14 or proHP21. These results indicate that PAP3, like PAP1, is a key factor of the self-reinforcing mechanism in the proPO activation system, which is linked to other immune responses in *M. sexta*.

Keywords

Insect immunity; hemolymph protein; serine proteinase cascade; clip domain; tobacco hornworm

1. Introduction

Vertebrates and invertebrates possess an innate immune system to fight off infection by opportunistic microbes in the environment. Although the system has gone through dramatic changes after divergence of animal groups, its theme remains more or less the same. For instance, extracellular serine proteinases (SPs) form cascade pathways to mediate antimicrobial responses upon tissue damage or pathogen invasion (Krem and Di Cera, 2002; Jiang and Kanost, 2000). In the human blood coagulation system, SPs known as clotting factors work together to trigger clot formation within minutes after wounding. Depending on

Send correspondence to: Haobo Jiang, Department of Entomology and Plant Pathology, Oklahoma State University, Stillwater, OK 74078, Telephone: (405)-744-9400, Fax: (405)-744-6039, haobo@okstate.edu.

stage, location and scale, positive and negative regulatory loops control potency and duration of this response. Thrombin activates its upstream clotting factors at first and, by binding to thrombomodulin, cleaves the same plasma factors at different sites to inactivate them at a later stage (Dahlback and Villoutreix, 2005). Serpins form covalent complexes with the clotting factors to regulate blood coagulation. Analogous SP cascades exist in arthropod hemolymph to mediate defense responses, and serpins modulate these processes. Positive feedback regulation also plays a role in insect embryonic development and innate immunity (Dissing et al., 2001; Wang and Jiang, 2008), both involving SP pathways.

The proteolytic activation of prophenoloxidase (proPO) is a humoral defense mechanism in insects and crustaceans (Ashida and Brey, 1998; Cerenius and Söderhäll, 2004). The zymogens are activated by proPO activating proteinases (PAPs), also known as PPAE or PPAF (Satoh et al., 1999; Jiang et al., 1998, 2003a and 2003b; Lee et al., 1998; Tang et al., 2006). In most insects studied so far, PAPs need one or two non-catalytic serine proteinase homologs (SPHs) to yield active phenoloxidases (POs) (Kwon et al., 2000; Yu et al., 2003; Park et al., 2010). POs produce reactive intermediates for melanin production, protein crosslinking, and microbe killing (Nappi and Christenson, 2005; Zhao et al., 2007 and 2011). The PAPs and SPHs, containing regulatory clip domain(s) at the amino terminus, are activated by an SP system (Kim et al. 2002; Gorman et al., 2007; Wang and Jiang, 2007; An et al., 2009). This system is initiated upon recognition of pathogen surface molecules by specific binding proteins. In the tobacco hornworm, *Manduca sexta* hemolymph proteinase-14 (HP14) precursor interacts with bacteria or fungi, autoactivates, and cleaves proHP21 (Ji et al., 2004; Wang and Jiang, 2006). Active HP21 then produces PAP2 and PAP3 (Gorman et al., 2007; Wang and Jiang, 2007), which generate active PO in the presence of two serine proteinase homologs (SPHs). Their precursors (proSPH1 and proSPH2) are not active as a cofactor for the PAPs until specific cleavages occur (Yu et al., 2003; Lu and Jiang, 2008). In the previous study, we discovered that a tiny amount of PAP1 led to a large increase in PO activity in plasma from naive *M. sexta* larvae: PAP1 somehow activated proHP6; HP6 activated proHP8 and proPAP1; HP8 activated spätzle precursor while PAP1 activated proPOs and proSPH2 (An et al., 2009 and 2010). To date, proSPH1 activating proteinase is not known in the tobacco hornworm. Neither is it clear if PAP1 is the major activator of proSPH2 or whether other regulatory loops exist in the SP system, for example, leading to the rapid generation of PAP2 and PAP3 in the early stage of melanization.

We have available a collection of HP cDNAs and their polyclonal antisera, which allows us to monitor changes in some of these HPs during immune responses and their regulation by serpins in the plasma (Jiang et al., 2005 and 2010). We now know that HP1, HP6, HP8, HP14, HP17, HP21, PAPs, SPH1, and SPH2 are probably involved in proPO and pro-spätzle activation. Serpin-1 variants and serpins 3 through 7 form covalent complexes with HPs (Ragan et al., 2010; Zhu et al., 2003; Christen et al., 2012; Tong et al., 2005; Zou et al., 2005; Suwanchaichinda et al., 2013). In this paper, we report the isolation of a major activating proteinase of proSPH1 and proSPH2 from hemolymph of pharate pupae and changes in the cell-free hemolymph from naïve and bacteria-injected larvae. Based on

immunoblot blot analyses of the plasma samples and *in vitro* tests using purified proteins, we propose new mechanisms that regulate proPO activation.

2. Methods and materials

2.1. Insect rearing, hemolymph collection, protein preparation and activity assays

M. sexta eggs were purchased from Carolina Biological Supply and hatched larvae were reared on an artificial diet (Dunn and Drake, 1983). Each of day 1, 5th instar larvae was injected with a mixture of *Escherichia coli* (1.3×10^7 cells), *Micrococcus luteus* (13 mg), and curdlan (13 mg, insoluble β-1,3-glucan from *Alcaligenes faecalis*) in 20 μl H_2O. Induced hemolymph (IH) was collected from cut prolegs of the larvae 24 h later and centrifuged at 14,000*g* for 5 min to remove hemocytes. Similarly, control hemolymph (CH) was collected from day 2, 5th instar naïve larvae. Aliquots of the cell-free CH and IH were stored at −80°C for use as a testing platform of proPO activation. PAP1 was purified from the cuticle extract (Gupta et al., 2005); PAP2 and PAP3 were isolated from hemolymph of bar-stage larvae (Jiang et al., 2003a and 2003b). The recombinant SPH1, SPH2, PAP1, PAP2, PAP3 and HP6 precursors were produced previously (Lu and Jiang, 2008; Ji et al., 2003; Gorman et al., 2007; Wang et al., 2001; Wang and Jiang, 2007 and 2008). ProPOs were isolated from plasma of feeding larvae as described by Jiang et al (1997). PO activity and acetyl-Ile-Glu-Ala-*p*-nitroanilide (IEAR*p*NA) hydrolysis were measured according to Jiang et al (2003a), with one unit defined as the amount of enzyme causing 0.001 unit of absorbance increase in one minute.

2.2. Collection, fractionation, and activation of hemolymph of bar stage insects

Pharate pupae with metathoracic brown bars were chilled on ice and dissected to collect bar stage hemolymph (BH). While gut and fat body tissues were removed from body wall with a spatula, pooled hemolymph was carefully collected using 1 ml pipette, avoiding contaminating tissue fragments, and immediately mixed with 100% saturated ammonium sulfate (pH 7.0) to suppress simultaneous melanization occurring at this developmental stage. The ammonium sulfate saturation was adjusted to 50% saturation prior to storage at −70°C. BH collected this way contained some active serine proteinases and their zymogens, which remained stable for at least two years. A frozen hemolymph sample (18 ml BH and 18 ml 100% ammonium sulfate) was thawed and centrifuged at 12,000*g* for 20 min to harvest precipitated proteins. The pellet was dissolved in 25 ml of HT buffer (pH 6.8, 10 mM potassium phosphate, 0.5 M NaCl), supplemented with 0.001% 1-phenyl-2-thiourea (PTU). After centrifugation at 15,000*g* for 30 min, ammonium sulfate saturation of the supernatant was raised to 35% and precipitated proteins were collected by centrifugation under the same conditions. The 0–35% ammonium sulfate fraction of BH was dissolved in 20 ml of HT buffer and the proPO activation system was further stimulated by incubating with 2 mg curdlan at room temperature for 10 min. The reaction mixture, supplemented with 0.5 mM *p*-aminobenzamidine, was dialyzed against HT buffer supplemented with 0.001% PTU and 0.5 mM benzamidine (1.0 L for 8 h, twice).

2.3. Purification of a proSPH processing enzyme

After flocculent substances including curdlan were removed by centrifugation at 15,000*g* for 30 min, the supernatant was applied to a hydroxylapatite column (2.5 cm i.d.×10 cm, Bio-Rad) equilibrated in HT buffer. Following a washing step with 100 ml HT buffer, bound proteins were eluted at 0.4 ml/min for 6 h with a linear gradient of 10–150 mM potassium phosphate (pH 6.8), 0.5 M NaCl (150 ml). Fractions (flow-through and washing, 8 ml/tube; elution, 4 ml/tube) that efficiently cleaved the proSPHs, hydrolyzed IEAR*p*NA, and had low A_{280nm} readings were pooled and precipitated by adding solid ammonium sulfate to a final saturation of 50%.

The protein precipitate, collected by centrifugation at 15,000*g* for 30 min, was dissolved in 3 ml of 20 mM Tris-HCl (pH 7.5), 0.5 M NaCl, supplemented with 0.001% PTU and 0.5 mM *p*-aminobenzamidine, and then resolved by gel filtration chromatography on a Sephacryl S100-HR column (2.5 cm i.d.×100 cm, Bio-Rad) equilibrated with the same buffer.

The highly active fractions (3 ml/tube) were combined, supplemented with 1 mM $CaCl_2$ and $MgCl_2$, and loaded onto concanavalin A-Sepharose (GE Healthcare Life Sciences) column (5.0 ml). Following a washing step, bound proteins were eluted from the lectin column with a linear gradient of 0–0.4 M methyl α-D-mannopyranoside in 30 ml of 20 mM Tris-HCl, pH 7.4, 0.5 M NaCl, 1 mM $CaCl_2$, 1 mM $MgCl_2$.

Pooled active fractions (1.5 ml/tube) were diluted 1:30 with 10 mM 2-[N-morpholino]ethane sulfonic acid, pH 6.4, 0.01% Tween-20 and applied to a dextran sulfate-Sepharose CL-6B column (5.0 ml). After washing with 30 ml of the buffer, a linear gradient of 0–1.0 M NaCl in 40 ml of the buffer was employed to elute proteins. Active fractions (1.5 ml each) were individually concentrated to 0.1 ml with Microcon-30 centrifugal filter units and stored at -80°C. Proteins in one of these fractions were precipitated with acetone and analyzed by nanoLC-MS/MS at OSU Recombinant DNA and Protein Core Facility.

2.4. Functional confirmation of PAP3 in the activation of proSPHs and proPOs

After the purified proSPH1, proSPH2, and both proSPHs were individually incubated with PAP3 and proPOs for 1 h on ice, PO activities were measured and plotted to test whether one SPH suffices to act as cofactor for proPO activation. Since the proSPH processing enzyme was not as pure as PAP3 isolated previously (Fig. 4D), we used the old preparation of PAP3 for all functional assays. The highly purified PAP3 was incubated with proSPH1 or proSPH2 for 1 h on ice to confirm its proSPH processing activity. In order to examine sizes of the cleavage products of the recombinant proSPHs and compare those of the SPH1 and SPH2 generated in plasma, IH and PAP3 were incubated for 15 min at room temperature. The reaction mixtures were subjected to 10% sodium dodecyl sulfate-polyacrylamide gel electrophoresis (SDS-PAGE), electrotransfer, and immunoblot analysis using diluted SPH1 or SPH-2 antiserum as the first antibody.

2.5. Determination of the PAP3 cleavage site in proSPH1

For cleavage site determination, proSPH1 (2 μg) was incubated with PAP3 (80 ng) in a 100 μl reaction mixture containing 20 mM Tris-HCl, pH 7.5, 0.001% Tween-20 on ice for 1 h.

After treatment with SDS sample buffer containing 2-mercaptoethanol, the reaction mixture was separated by 10% SDS-PAGE under reducing condition. Proteins were then transferred to a polyvinylidene difluoride membrane, lightly stained with Coomassie Brilliant Blue R-250 (Sigma). The 38 kDa polypeptide was subjected to automated Edman degradation at UC Davis Proteomics Core Facility.

2.6. PAP3-stimulated proPO activation in plasma from naïve and immune challenged larvae

In order to test if PAP3, like PAP1 in CH, is able to greatly enhance proPO activation in plasma, CH and IH samples were separately mixed with buffer, the purified cofactor (*i.e*. SPHs), PAP1, or PAP3 at room temperature for 15 min. As controls, proPOs alone and proPO activation mixture (proPOs, SPHs, PAP3 and buffer) were incubated on ice for 1 h prior to PO activity measurement.

2.7. Immunoblot analysis of proHP, proSPH and proPO proteolysis in the plasma

CH and IH samples from naïve and bacteria-injected larvae were individually incubated at room temperature for 15 min with buffer or PAP3 in the presence of 0.01% PTU. After treatment with SDS sample buffer containing 2-mercaptoethanol, the samples (equivalent to 2 μl plasma) were resolved by SDS-PAGE. Following electrotransfer and blocking, the protein blots were individually reacted with 1:2,000 diluted polyclonal antisera against SPH1, SPH2, PAP1, PAP3, SPH1, SPH2, PO2, HP1, HP2, HP6, HP8, HP14, HP16, HP17, HP19, and HP21. The antigen-antibody complexes were visualized by a color reaction catalyzed by 1:2000 diluted alkaline phosphatase conjugated to goat-anti-rabbit IgG (Bio-Rad).

2.8. Possible cleavage of the purified proPAP1, proHP6, and proPAP3 by PAP3

The recombinant proPAP1, proHP6, and proPAP3 were incubated with highly purified PAP3 at room temperature for 1 h. In the negative controls, the same amounts of proenzymes and PAP3 were separately incubated with buffer under the same conditions. The reaction mixtures were subjected to SDS-PAGE and immunoblot analysis. In order to test if proPAP3 activated by PAP3 could generate additional IEARase activity, proPAP3, PAP3, and a mixture of the same amounts of proPAP3 and PAP3 were incubated at room temperature for 1 h, the amidase activities were determined as described in *Section 2.1*.

3. Results and discussion

3.1. Purification of a proSPH processing enzyme

In order to isolate the hemolymph proteinase that activates *M. sexta* proSPH1 and proSPH2, we fractionated the plasma from bar-stage larvae with 0–35% saturated ammonium sulfate and stimulated the proPO activation system in this fraction with curdlan, which mimics fungal infection. Following a dialysis step, the protein sample was separated by hydroxyapatite chromatography, and the fractions were individually incubated with the recombinant proSPH1 or proSPH2 (Lu and Jiang, 2008) to monitor their processing. Since the proSPHs were cleaved next to an Arg (Yu et al., 2003; Wang and Jiang, 2004), we also used IEAR*p*NA to measure the amidase activity which may correlate with the proSPH

activating proteinase, especially in later stages of the purification. Fractions 10 through 30 contained low levels of proteins but efficiently processed the proSPHs (Fig. 1). The activity overlapped with a major amidase activity peak that hydrolyzed IEAR*p*NA. Since the minor IEARase peak around fraction 31 did not cause a noticeable increase in the SPH precursor cleavage, we combined the fractions 11–26 and, by avoiding contaminants in the fractions 10 and 27–30, largely reduced complexity of the pooled sample (data not shown). After ammonium sulfate precipitation, we resolved the resolubilized proteins by gel filtration chromatography. A_{280nm} readings were low in most of the fractions (Fig. 2) and there was an IEARase activity peak in fractions 40–46, correlating with the proSPH processing activity. After the combined fractions were loaded onto a concanavalin A-Sepharose column, half of the proteins did not bind (data not shown); the IEARase and proSPH processing activities were detected in the same bound fractions (Fig. 3). We finally separated the eluted proteins in fractions 5–7 by cation exchange chromatography on a dextran sulfate column. The IEARase activity again correlated with the proSPH processing activity and a two-chain protein (Fig. 4) in fractions 6–9. Immunoblot analysis using the HP antibodies (Jiang et al., 2005) indicated this protein is PAP3. LC-MS/MS analysis of the protein sample showed PAP3 was the only HP in the sample.

3.2. Functional confirmation of the proSPH processing enzyme in proPO activation

Our previous studies demonstrated that PAP3 activated proPO in the presence of a cofactor of SPH1 and SPH2 (Jiang et al., 2003b). Since PAP3 processed the proSPHs, we tested if the cleavage products are active as a cofactor for PAP3 to activate proPO. Incubation of highly purified PAP3 (Fig. 4D) with proSPH1 and proPO did not yield PO activity (Fig. 5). Neither did the proSPH2 cleavage product assist PAP3 in producing active PO. However, after PAP3, proSPH1, proSPH2, and proPOs were present in the same reaction mixture, the cleaved SPHs acted as an auxiliary factor for PAP3-mediated proPO activation. These results are consistent with an earlier observation that co-presence of the SPH1 and SPH2 is necessary for the cofactor activity (Lu and Jiang, 2008).

The proteolytic cleavage of proSPHs is a complex process worth investigating. The SPHs isolated from induced hemolymph of feeding larvae were somewhat different from those in BH (Wang and Yang, 2004). While the 31 kDa SPH1 and 37 kDa SPH2 were generated by cleavage next to Arg^{133} and Arg^{77} respectively (Yu et al., 2003), nearly half of the proSPH1 in the plasma of bar stage insects was cut at an undetermined site before Arg^{84} (Wang and Yang, 2005). Here we showed that PAP3 cleaved recombinant proSPHs to generate 38 kDa bands mainly (Figs. 1–5) – the additional 1 kDa may come from the carboxyl-terminal affinity tag (Lu and Jiang, 2008). Based on the results of proPO activation (Fig. 5), we concluded that the complex of 37/38 kDa SPH1 and SPH2, like the complex of 31 kDa SPH1 and 37 kDa SPH2 in IH, was active as PAP cofactor (Fig. 5). To better characterize the activation of proSPH1 by PAP3, we determined the N-terminal sequence of the 38 kDa band as Phe^{83}-Arg-Gly-Asp-Pro, indicating that the scissile bond is between Arg^{82} and Phe^{83}in the clip domain. This result agreed with our prediction based on the fact that PAP3 cuts both proPO1 and proPO between Arg^{51} and Phe^{52}. The 38 kDa SPH2 also started at Phe^{78} (Yu et al., 2003). We noticed other cleavage products: 32 kDa SPH1 (Arg^{133}*Thr^{133}), 25 kDa SPH1, and 25 kDa SPH2 bands (Fig. 4), but failed to identify the minor cleavage

sites (*) in the latter two due to their low levels. Further mutation analysis is necessary to test if there is any quantitative difference in the cofactor activity between the 32 and 38 kDa SPH1 in complex with the 38 kDa SPH2.

3.3. PAP3 at low concentration strongly stimulates the proPO activation system in larval plasma

In the previous work, addition of a minute amount of PAP1 to naïve larval hemolymph (CH) greatly enhanced proPO activation, even though purified PAP1 can only activate a small quantity of proSPH2 and proPOs (Wang and Jiang, 2008). Further experiments led to the discovery of a positive feedback mechanism that generates HP6, HP8, PAP1, SPH1, SPH2 and PO2 in plasma. Since PAP3 yields active SPHs and POs (Fig. 5), we tested if it may also substantially stimulate the proPO activation system. While proPOs only and proPOs in cell-free hemolymph (CH or IH) had little PO activity, adding 20 ng PAP3 to the plasma samples (2.0 μl) remarkably enhanced the proPO activation (150 U in CH and 100 U in IH) (Fig. 6). The activity levels were even higher than that caused by PAP1 (60 U in CH and 10 U in IH). In another control, incubation of 100 ng proPOs, 20 ng SPHs, and 20 ng PAP3 yielded 30 U PO, considerably lower than 150 or 100 U. The PAP3 level in the CH and IH was also minimal and lower than that in the control, since adding 20 ng SPHs to CH or IH failed to generate much active PO (Fig. 6). In other words, the actual PO activity differences between the control (30 U) and tests (100 and 150 U) was even larger than they appeared (70 and 120 U). PAP3, like PAP1 in CH, did cause a drastic increase in PO activity beyond its own ability to activate proPOs via proteolysis.

3.4. Changes accompanying the enhancement of proPO activation

While part of the enhancement is expected to be caused by the proSPH processing activity of PAP3, were there any other changes in CH or IH which may also account for the major increases? We, therefore, used our collection of HP antisera to probe cleavage events concurring with the proPO activation. First of all, after PAP3 was added to CH or IH, all proSPH1 and most proSPH2 was converted to 37 kDa bands (Fig. 7, A & B), which were tethered to their respective light chains (calculated M_r: ~8.5 kDa) via three disulfide bonds in the clip domains (Yu et al., 2003). The disulfide linkages between Cys-1 and Cys-5, Cys-2 and Cys-4, and Cys-3 and Cys-6 in the known clip domain structures (Huang et al., 2007; Piao et al., 2005) and cleavage of the peptide bond in the region between Cys-3 and Cys-4 did not affect the tethering of light and heavy chains. Secondly, all proPAP1 in CH and a small portion of proPAP1 in IH became PAP1, whose 31 kDa catalytic domain was hardly detected by the PAP1 antibodies (Fig. 7, C and C'). Like proPAP1, proPAP3 levels in IH were much higher than those in CH. In response to the added PAP3, nearly all the proPAP3 became active, and its catalytic heavy chain may have formed SDS-stable complexes with serpins (Fig. 7, D and D') (Christen et al., 2012; Zou and Jiang, 2005; Suwanchaichinda et al., 2013). The presence of PAP1, PAP3, SPH1 and SPH2 apparently caused proteolytic activation of proPO2 (Fig. E) and proPO1 (data not shown) – the antibodies against proPOs isolated from the larval hemolymph cross-reacted with other plasma proteins. Thirdly, PAP3 as well as PAP1 (Wang and Jiang, 2008) somehow activated proHP6. Active HP6 then cleaved proHP8 and proPAP1 to generate HP8 and PAP1, respectively (An et al., 2009) (Fig. 7, F and G). An SDS-stable complex (~70 kDa) of HP6

and another protein was detected in IH, suggesting that serpin-4 and serpin-5 probably inhibited active HP6 (Tong et al., 2005) – formation of an acyl complex with the active site Ser in the protease domain is a unique feature of serpin. While a similar amount of proHP6 disappeared due to processing, less ~70 kDa complex was detected in CH due to the lower serpin levels. Instead, significant amount of the 28 kDa catalytic domain of HP6 was detected (Fig. 7F). The regulatory light chain of HP6 was hardly recognized by the antibodies. Interestingly, while proPAP3 in CH and IH was activated, neither HP14 nor HP21 was activated (data not shown). Since HP14 activates proHP21 and HP21 activates proPAP2 and proPAP3 (Wang and Jiang, 2007; Gorman et al., 2007), the observed proPAP3 activation did not go through HP14 or HP21. Addition of PAP3 did not lead to significant cleavage of proHP1, proHP2, proHP16, proHP17 or proHP19 (data not shown).

3.5. PAP3 cleaves purified proPAP1, proHP6, and proPAP3

PAP1 cleaved the recombinant proHP6 and proHP8 *in vitro* but the products differ from HP6 and HP8 produced in plasma in response to the exogenous PAP1 (Wang and Jiang, 2008). The correctly processed HP6 activates proPAP1 to generate more PAP1 and, thus, form a positive feedback loop. To examine whether PAP3 could directly activate proPAP1 or proHP6, we incubated purified PAP3 with the proPAP1 or proHP6 and detected possible cleavage by immunoblot analysis. Since proPAP1 and proHP6 remained intact (Fig. 8, A and B), the partial activation of proPAP1 (Fig. 7, C and C') and proHP6 (Fig. 7F) in plasma by exogenous PAP3 appeared to be indirect.

Since the proPAP3 activation (Fig. 7, D and D') was not through HP14 or HP21 (data not shown), we tested if PAP3 could directly activate proPAP3. To our surprise, PAP3 completely converted proPAP3 to 37 and 19 kDa bands (Fig. 8C), consistent in size with the heavy and light chains of PAP3 (Jiang et al., 2003b). IEARase activity of the reaction mixture became much higher than PAP3 alone. We repeated the same test with three other batches of the recombinant proPAP3 and also observed major increases in IEARase activity (data not shown). By activating its own zymogen to generate a large amount of PAP3 and by activating the proSPHs to become its own cofactor, PAP3 activated proPOs more efficiently (Fig. 6). While these two mechanisms have experimental supports, it is possible other plasma factors have also contributed to the boost of proPO activation.

3.6. Multiple functions of PAP3 in proPO activation

Like PAP1 and PAP2, PAP3 activates proPO in the presence of SPH1 and SPH2 (Jiang et al., 1998, 2003a, 2003b; Yu et al., 2003). We named them PAPs to distinguish from *Bombyx mori* proPO activating enzyme (PPAE) (Satoh et al., 1999), which generates active PO by itself, and considered *M. sexta* PAP1/2/3 as the catalytic component of PPAE. For a long time, we thought the PAPs have only one function by cleaving the proPOs between Arg^{51} and Phe^{52}. This simple picture changed after we had discovered PAP1 somehow activated proHP6 and, through HP6, activated proHP8 and proPAP1 (Wang and Jiang, 2008). PAP1 efficiently activated proSPH2, and although proSPH1 activation by PAP1 was below the detection limit, incubation of PAP1 with proSPH1, proSPH2, and proPOs generated PO activity significantly higher than the sum of PO activities in the PAP1-proSPH1-proPOs and PAP1-proSPH2-proPOs reactions (Wang and Jiang, 2008). In this study, we demonstrated

that *M. sexta* PAP3 is the major enzyme in bar stage hemolymph that cleaves proSPH1 between Arg^{82} and Phe^{83} and proSPH2 between Arg^{77} and Phe^{88}. We now conclude that both PAP3 and PAP1 (to a lesser extent) function as activating proteinases of proSPH-1 and proSPH-2 (Fig. 9). While it is not understood why three PAPs exist in *M. sexta*, the genome analysis suggests that the rapid expansion of dual clip-domain serine proteinase genes is responsible for the emergence of PAP2 and PAP3 (unpublished data). Further biochemical study is needed to test if PAP2 has similar functions and how these three enzymes may complement each other in stimulating melanization.

M. sexta is not the only insect whose PAPs generate their own cofactor for proPO activation. In *Tenebrio molitor*, spätzle processing enzyme (SPE) cleaves proSPH1, proPO, and pro-spätzle (Kan et al., 2008; Roh et al., 2009). While SPE activates proPO in the presence of SPH1 for melanization, it also produces spätzle for Toll pathway activation in the beetle. In *M. sexta*, HP8 specifically activates pro-spätzle (An et al., 2010) and addition of PAP1 or PAP3 may indirectly activate HP8 and spätzle to stimulate the Toll pathway. Perhaps, the most important finding of this work is the direct positive feedback mechanism of PAP3-mediated proPAP3 activation (Fig. 9), previously not known to exist in any insect immune proteinase pathways. Unlike the indirect activation of proPAP1 by PAP1 through HP6 (Wang and Jiang, 2008), the production of PAP3 at least partially explained why such a dramatic enhancement in proPO activation (Fig. 6) occurred, far beyond the capability of the added PAP3 in generating the SPHs and POs. The potential danger of converting all proPAP3 to PAP3 calls for tight regulation by serpin-3 (Christen et al., 2012), serpin-6 (Zou and Jiang, 2005), and serpin-7 (Suwanchaichinda et al., 2013).

3.7. Concluding remarks

M. sexta is a useful model for biochemical research on insect immune responses (Jiang et al., 2010). Among these responses, proPO activation and melanization represents one of the most thoroughly studied immune processes in arthropods. Here we have discovered that PAP3 is the major activating proteinase of proSPH1 and proSPH2 in the plasma from the bar stage larvae. PAP3 generates active SPH1 and SPH2, which then function as a cofactor with PAP3 for proPO activation (Fig. 9). Proteolytic cleavage of all four precursor proteins by PAP3 occurs between Arg and Phe. In the presence of unknown plasma factors, a small amount of PAP3 leads to the activation of HP6, HP8, PAP1, and PAP3 zymogens in hemolymph. The direct activation of proPAP3 by PAP3 greatly increases the proSPH and proPO activation, which represent another positive feedback mechanism discovered in this insect. Unlike porPO activation, autoactivation of proPAP3 is SPH-independent.

Acknowledgments

We thank Dr. Michael Kanost for his helpful comments on the manuscript. This work was supported by National Institutes of Health Grant GM58634 (to HJ). We would like to thank Dr. Gorman for the generous gift of purified recombinant proPAP3. This article was approved for publication by the Director of Oklahoma Agricultural Experimental Station and supported in part under project OKLO2450.

Abbreviations

PO and proPO	phenoloxidase and its precursor
HP	hemolymph proteinase
SP and SPH	serine proteinase and its non-catalytic homolog
PAP (PPAE or PPAF)	proPO activating proteinase (enzyme or factor)
IEAR*p*NA and IEARase, SPE	spätzle processing enzyme; acetyl-Ile-Glu-Ala-Arg-*p*-nitroanilide and its hydrolyzing enzyme
SDS-PAGE	sodium dodecyl sulfate-polyacrylamide gel electrophoresis
BH	bar stage larval hemolymph
CH	control hemolymph from naïve larvae
IH	induced hemolymph from bacteria-injected larvae
PTU	1-phenyl-2-thiourea
LC-MS/MS	liquid chromatography-tandem mass spectrometry

References

An C, Ishibashi J, Ragan EJ, Jiang H, Kanost MR. Functions of *Manduca sexta* hemolymph proteinases HP6 and HP8 in two innate immune pathways. J Biol Chem. 2009; 284:19716–19726. [PubMed: 19487692]

An C, Jiang H, Kanost MR. Proteolytic activation and function of the cytokine Spätzle in innate immune response of a lepidopteran insect, *Manduca sexta*. FEBS J. 2010; 277:148–162. [PubMed: 19968713]

Ashida, M.; Brey, PT. Recent advances on the research of the insect prophenoloxidase cascade. In: Brey, PT.; Hultmark, D., editors. Molecular Mechanisms of Immune Responses in Insects. London: Chapman & Hall; 1998. p. 135-172.

Cerenius L, Söderhäll K. The prophenoloxidase-activating system in invertebrates. Immunol Rev. 2004; 198:116–126. [PubMed: 15199959]

Christen JM, Hiromasa Y, An C, Kanost MR. Identification of plasma proteinase complexes with serpin-3 in *Manduca sexta*. Insect Biochem Mol Biol. 2012; 42:946–955. [PubMed: 23063421]

Dahlback B, Villoutreix BO. The anticoagulant protein C pathway. FEBS Lett. 2005; 579:3310–3316. [PubMed: 15943976]

Dissing M, Giordano H, DeLotto R. Autoproteolysis and feedback in a protease cascade directing *Drosophila* dorsal-ventral cell fate. EMBO J. 2001; 20:2387–2393. [PubMed: 11350927]

Dunn P, Drake D. Fate of bacteria injected into naïve and immunized larvae of the tobacco hornworm, *Manduca sexta*. J Invert Pathol. 1983; 41:77–85.

Gorman MJ, Wang Y, Jiang H, Kanost MR. *Manduca sexta* hemolymph proteinase 21 activates prophenoloxidase activating proteinase 3 in an insect innate immune response proteinase cascade. J Biol Chem. 2007; 282:11742–11749. [PubMed: 17317663]

Gupta S, Wang Y, Jiang H. Purification and characterization of *Manduca sexta* prophenoloxidase-activating proteinase-1 (PAP-1), an enzyme involved in insect immune responses. Protein Exp Purif. 2005; 39:261–268.

Huang R, Lu Z, Dai H, Vander Velde D, Prakash O, Jiang H. The solution structure of the clip domains from *Manduca sexta* prophenoloxidase activating proteinase-2. Biochemistry. 2007; 46:11431–11439. [PubMed: 17880110]

Ji C, Wang Y, Guo X, Hartson S, Jiang H. A pattern recognition serine proteinase triggers the prophenoloxidase activation cascade in the tobacco hornworm, *Manduca sexta*. J Biol Chem. 2004; 279:34101–34106. [PubMed: 15190055]

Ji C, Wang Y, Ross J, Jiang H. Expression and *in vitro* activation of *Manduca sexta* prophenoloxidase-activating proteinase-2 precursor (proPAP-2) from baculovirus-infected insect cells. Protein Express Purif. 2003; 29:235–243.

Jiang H, Kanost MR. The clip-domain family of serine proteinases in arthropods. Insect Biochem Mol Biol. 2000; 30:95–105. [PubMed: 10696585]

Jiang, H.; Vilcinskas, A.; Kanost, MR. Immunity in lepidopteran insects. In “Invertebrate Immunity”. In: Söderhäll, K., editor. Adv Exp Med Biol. Vol. 708. 2010. p. 181-204.

Jiang H, Wang Y, Gu Y, Guo X, Zou Z, Scholz F, Trenczek TE, Kanost MR. Molecular identification of a bevy of serine proteinases in *Manduca sexta* hemolymph. Insect Biochem Mol Biol. 2005; 35:931–943. [PubMed: 15944088]

Jiang H, Wang Y, Kanost MR. Prophenoloxidase activating proteinase from an insect, *Manduca sexta*: a bacteria-inducible protein similar to *Drosophila* easter. Proc Natl Acad Sci USA. 1998; 95:12220–12225. [PubMed: 9770467]

Jiang H, Wang Y, Ma C, Kanost MR. Subunit composition of prophenoloxidase from *Manduca sexta*: molecular cloning of subunit proPO-p1. Insect Biochem Mol Biol. 1997; 27:835–850. [PubMed: 9474780]

Jiang H, Wang Y, Yu X-Q, Kanost MR. Prophenoloxidase-activating proteinase-2 (PAP-2) from hemolymph of *Manduca sexta*: a bacteria-inducible serine proteinase containing two clip domains. J Biol Chem. 2003a; 278:3552–3561. [PubMed: 12456683]

Jiang H, Wang Y, Yu X-Q, Zhu Y, Kanost MR. Prophenoloxidase-activating proteinase-3 (PAP-3) from *Manduca sexta* hemolymph: a clip-domain serine proteinase regulated by serpin-1J and serine proteinase homologs. Insect Biochem Mol Biol. 2003b; 33:1049–1060. [PubMed: 14505699]

Kan H, Kim CH, Kwon HM, Park JW, Roh KB, Lee H, Park BJ, Zhang R, Zhang J, Söderhäll K, Ha NC, Lee BL. Molecular control of phenoloxidase-induced melanin synthesis in an insect. J Biol Chem. 2008; 283:25316–25323. [PubMed: 18628205]

Kim MS, Baek MJ, Lee MH, Park JW, Lee SY, Söderhäll K, Lee BL. A new easter-type serine protease cleaves a masquerade-like protein during prophenoloxidase activation in *Holotrichia diomphalia* larvae. J Biol Chem. 2002; 277:39999–40004. [PubMed: 12185078]

Krem MM, Di Cera E. Evolution of enzyme cascades from embryonic development to blood coagulation. Trends Biochem Sci. 2002; 27:67–74. [PubMed: 11852243]

Kwon TH, Kim MS, Choi HW, Joo MY, Lee BL. A masquerade-like serine proteinase homologue is necessary for phenoloxidase activity in the coleopteran insect, *Holotrichia diomphalia* larvae. Eur J Biochem. 2000; 267:6188–6196. [PubMed: 11012672]

Lee SY, Kwon TH, Hyun JH, Choi JS, Kawabata SI, Iwanaga S, Lee BL. *In vitro* activation of prophenoloxidase by two kinds of prophenoloxidase-activating factors isolated from hemolymph of coleopteran, *Holotrichia diomphalia* larvae. Eur J Biochem. 1998; 254:50–57. [PubMed: 9652393]

Lu Z, Jiang H. Expression of *Manduca sexta* serine proteinase homolog precursors in insect cells and their proteolytic activation. Insect Biochem Mol Biol. 2008; 38:89–98. [PubMed: 18070668]

Nappi AJ, Christensen BM. Melanogenesis and associated cytotoxic reactions: applications to insect innate immunity. Insect Biochem Mol Biol. 2005; 35:443–459. [PubMed: 15804578]

Park, JW.; Kim, CH.; Rui, J.; Park, KH.; Ryu, KH.; Chai, JH.; Hwang, HO.; Kurokawa, K.; Ha, NC.; Söderhäll, I.; Söderhäll, K.; Lee, BL. Beetle immunity. In “Invertebrate Immunity”. In: Söderhäll, K., editor. Adv Exp Med Biol. Vol. 708. 2010. p. 163-180.

Piao S, Song YL, Kim JH, Park SY, Park JW, Lee BL, Oh BH, Ha NC. Crystal structure of a clip-domain serine protease and functional roles of the clip domains. EMBO J. 2005; 24:4404–4414. [PubMed: 16362048]

Ragan EJ, An C, Yang CT, Kanost MR. Analysis of mutually exclusive alternatively spliced serpin-1 isoforms and identification of serpin-1 proteinase complexes in *Manduca sexta* hemolymph. J Biol Chem. 2010; 285:29642–29650. [PubMed: 20624920]

Roh KB, Kim CH, Lee H, Kwon HM, Park JW, Ryu JH, Kurokawa K, Ha NC, Lee WJ, Lemaitre B, Söderhäll K, Lee BL. Proteolytic cascade for the activation of the insect toll pathway induced by the fungal cell wall component. J Biol Chem. 2009; 284:19474–19481. [PubMed: 19473968]

Satoh D, Horii A, Ochiai M, Ashida M. Prophenoloxidase-activating enzyme of the silkworm, *Bombyx mori*: purification, characterization and cDNA cloning. J Biol Chem. 1999; 274:7441–7453. [PubMed: 10066809]

Suwanchaichinda C, Ochieng R, Zhuang S, Kanost MR. *Manduca sexta* serpin-7, a putative regulator of hemolymph prophenoloxidase activation. Insect Biochem Mol Biol. 2013; 43:555–561. [PubMed: 23567587]

Tang H, Kambris Z, Lemaitre B, Hashimoto C. Two proteases defining a melanization cascade in the immune system of *Drosophila*. J Biol Chem. 2006; 281:28097–28104. [PubMed: 16861233]

Tong Y, Jiang H, Kanost MR. Identification of plasma proteases inhibited by *Manduca sexta* serpin-4 and serpin-5 and their association with components of the prophenol oxidase activation pathway. J Biol Chem. 2005; 280:14932–14942. [PubMed: 15695806]

Wang Y, Jiang H, Kanost MR. Expression and purification of *Manduca sexta* prophenoloxidase-activating proteinase precursor (proPAP) from baculovirus-infected insect cells. Protein Express Purif. 2001; 23:328–337.

Wang Y, Jiang H. Prophenoloxidase (proPO) activation in *Manduca sexta*: an analysis of molecular interactions among proPO, proPO-activating proteiase-3, and a cofactor. Insect Biochem Mol Biol. 2004; 34:731–742. [PubMed: 15262278]

Wang Y, Jiang H. Interaction of β-1,3-glucan with its recognition protein activates hemolymph proteinase 14, an initiation enzyme of the prophenoloxidase activation system in *Manduca sexta*. J Biol Chem. 2006; 281:9271–9278. [PubMed: 16461344]

Wang Y, Jiang H. Reconstitution of a branch of *Manduca sexta* prophenoloxidase activation cascade *in vitro*: Snake-like hemolymph proteinase 21 cleaved by HP14 activates prophenoloxidase-activating proteinase-2 precursor. Insect Biochem Mol Biol. 2007; 37:1015–1025. [PubMed: 17785189]

Wang Y, Jiang H. A positive feedback mechanism in the *Manduca sexta* prophenoloxidase activation. Insect Biochem Mol Biol. 2008; 38:763–769. [PubMed: 18625399]

Yu XQ, Jiang H, Wang Y, Kanost MR. Nonproteolytic serine protease homologs are involved in prophenoloxidase activation in the tobacco hornworm, *Manduca sexta*. Insect Biochem Mol Biol. 2003; 33:197–208. [PubMed: 12535678]

Zhao P, Li J, Wang Y, Jiang H. Broad-spectrum antimicrobial activity of the reactive compounds generated *in vitro* by *Manduca sexta* phenoloxidase. Insect Biochem Mol Biol. 2007; 37:952–959. [PubMed: 17681234]

Zhao P, Lu Z, Strand M, Jiang H. Antiviral, antiparasitic, and cytotoxic effects of 5,6-dihydroxyindole (DHI), a reactive compound generated by phenoloxidase during insect immune response. Insect Biochem Mol Biol. 2011; 41:645–652. [PubMed: 21554953]

Zhu Y, Wang Y, Gorman M, Jiang H, Kanost MR. *Manduca sexta* serpin-3 regulates prophenoloxidase activation in response to infection by inhibiting prophenoloxidase-activating proteinases. J Biol Chem. 2003; 47:46556–46564. [PubMed: 12966082]

Zou Z, Jiang H. *Manduca sexta* serpin-6 regulates immune serine proteinases PAP-3 and HP8: cDNA cloning, protein expression, inhibition kinetics, and function elucidation. J Biol Chem. 2005; 280:14341–14348. [PubMed: 15691825]

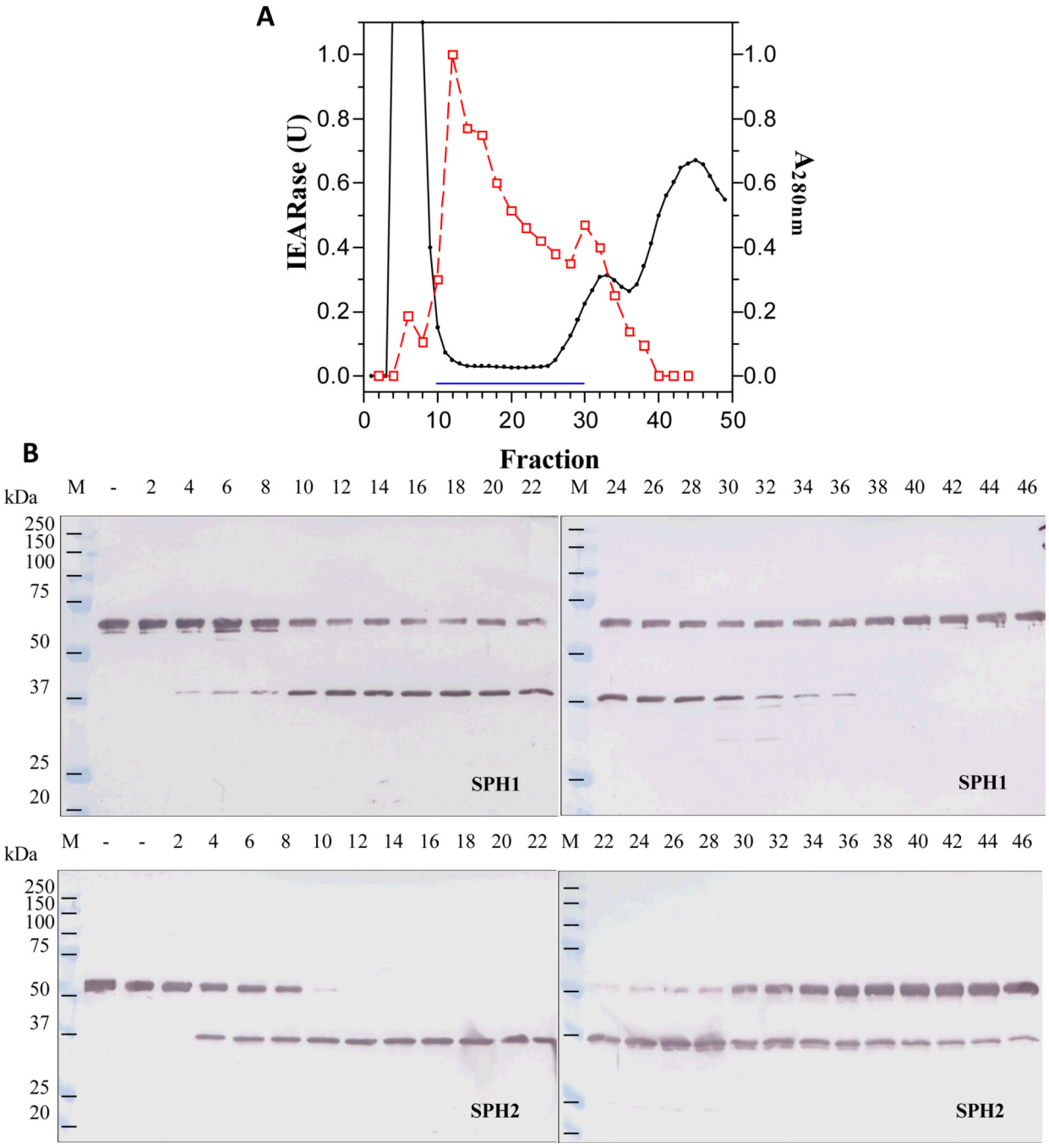

Fig. 1. Separation of an ammonium sulfate fraction of the bar stage hemolymph by hydroxylapatite chromatography (A) and detection of a proSPH activating enzyme activity in the fractions by immunoblot analysis (B)

As described in *Sections 2.2* and *2.3*, 18 ml of BH was fractionated with 0–35% ammonium sulfate, activated by β-1,3-glucan, and resolved on a hydroxylapatite column. Amidase activities in 10 μl fractions were measured in a microplate assay using 200 μl of 50 μM IEAR*p*NA in 0.1 M Tris-HCl, 0.1 M NaCl, 5 mM $CaCl_2$, pH 7.8 (Jiang et al., 2003a). Column fractions (1 μl each) were incubated with proSPH1 or proSPH2 (200 ng, 1 μl) and 20 mM Tris-HCl, pH 7.5, 0.001% Tween-20 (10 μl) on ice for 1 h. The reaction mixtures

were subjected to 10% SDS-polyacrylamide gel electrophoresis (PAGE) and immunoblot analysis using 1:2,000 diluted SPH1 or SPH2 antiserum as the first antibody. Panel A: A_{280nm} (•——•); IEARase activity (□ - - □); proSPH processing (——); pooled fractions (#11-#26). Panel B: sizes and positions of the marker proteins (M), fraction numbers, proSPHs, and antibodies are indicated.

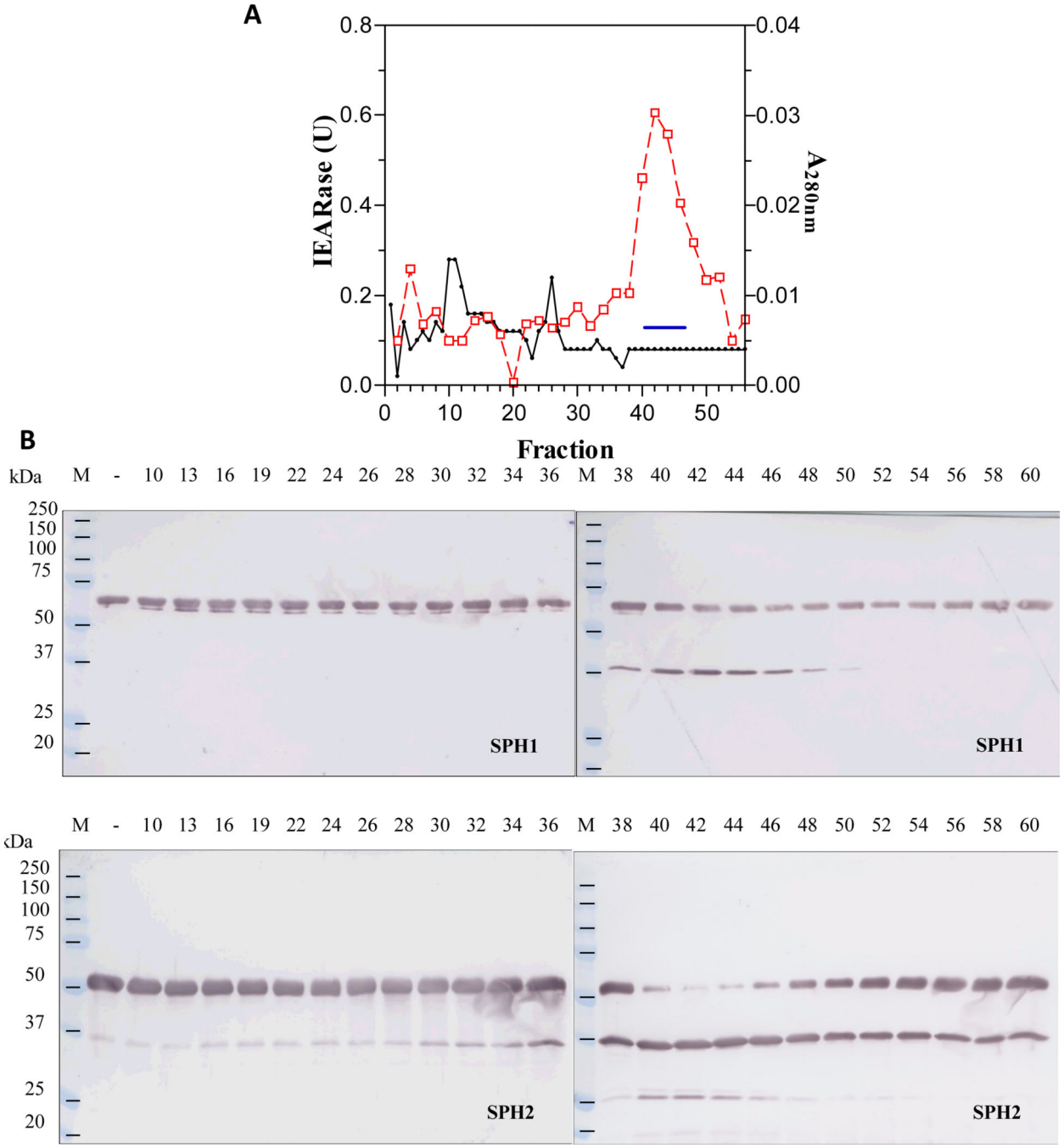

Fig. 2. Separation of the pooled hydroxylapatite fractions by gel filtration chromatography (A) and detection of proSPH processing by the column fractions (B)

As described in *Section 2.3*, proteins in the flow-through fractions (#11-#26) were precipitated with solid ammonium sulfate, dissolved in 3 ml buffer, and resolved on a Sephacryl S100-HR column. IEARase activities in 10 μl fractions, A_{280nm} values, and proSPH processing by the fractions (2 μl each) were measured and shown as described in Fig. 1 legend.

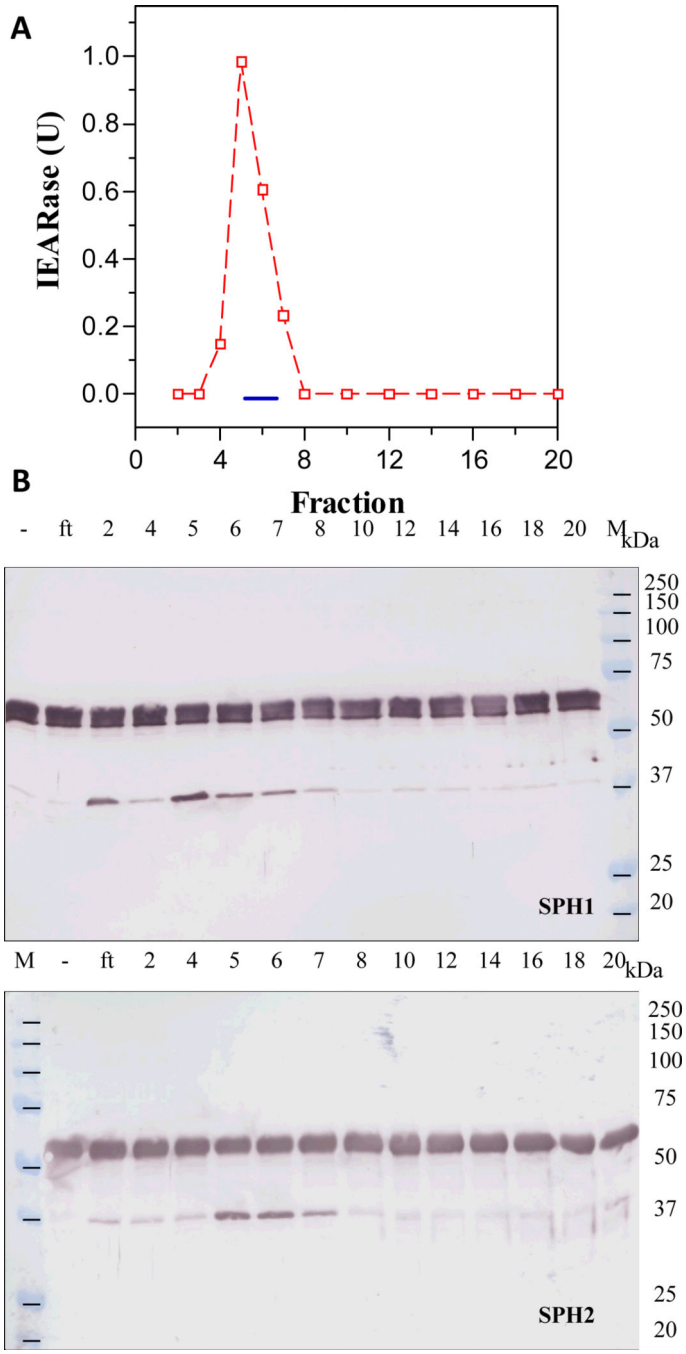

Fig. 3. Separation of the combined S100 fractions by lectin affinity chromatography (A) and detection of the proSPH activating enzyme activity in the bound fractions (B)

As described in *Section 2.3*, the combined S100 fractions (#40-#46) were replenished with $CaCl_2$ and $MgCl_2$ and loaded onto a concanavalin A column. IEARase activities in 10 μl fractions and proSPH processing by the fractions (1 μl each) were measured as described in Fig. 1 legend.

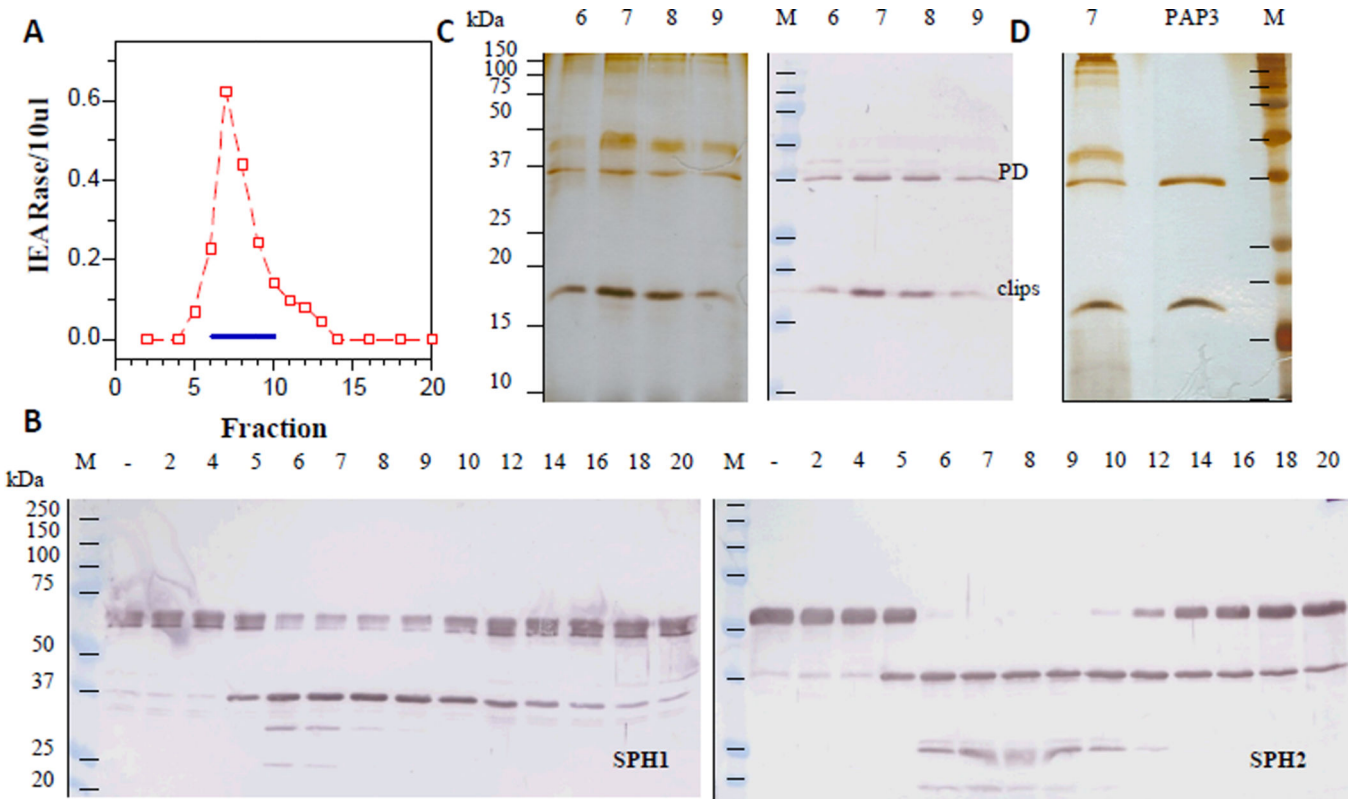

Fig. 4. Separation of the pooled concanavalin A fractions by ion exchange chromatography (A) and detection of proSPH enzyme activity (B) and proteins (C and D) in the fractions

As described in *Section 2.3*, the lectin-bound fractions (#5–#7) were diluted and separated on a dextran sulfate-Sepharose column. IEARase activities in 10 μl fractions (panel A) and proSPH processing by the fractions (5 μl each) (panel B) were measured and shown as described in Fig. 1 legend. Panel C: individually concentrated fractions #6–#9 (10 μl each) were subjected to 12% SDS-PAGE followed by silver staining (*left*) or immunoblotting (*right*) using 1:3000 diluted PAP3 antiserum as the first antibody. Panel D: comparison of the concentrated fraction #7 (12 μl) and highly purified PAP3 (60 ng) (Jiang et al., 2003b).

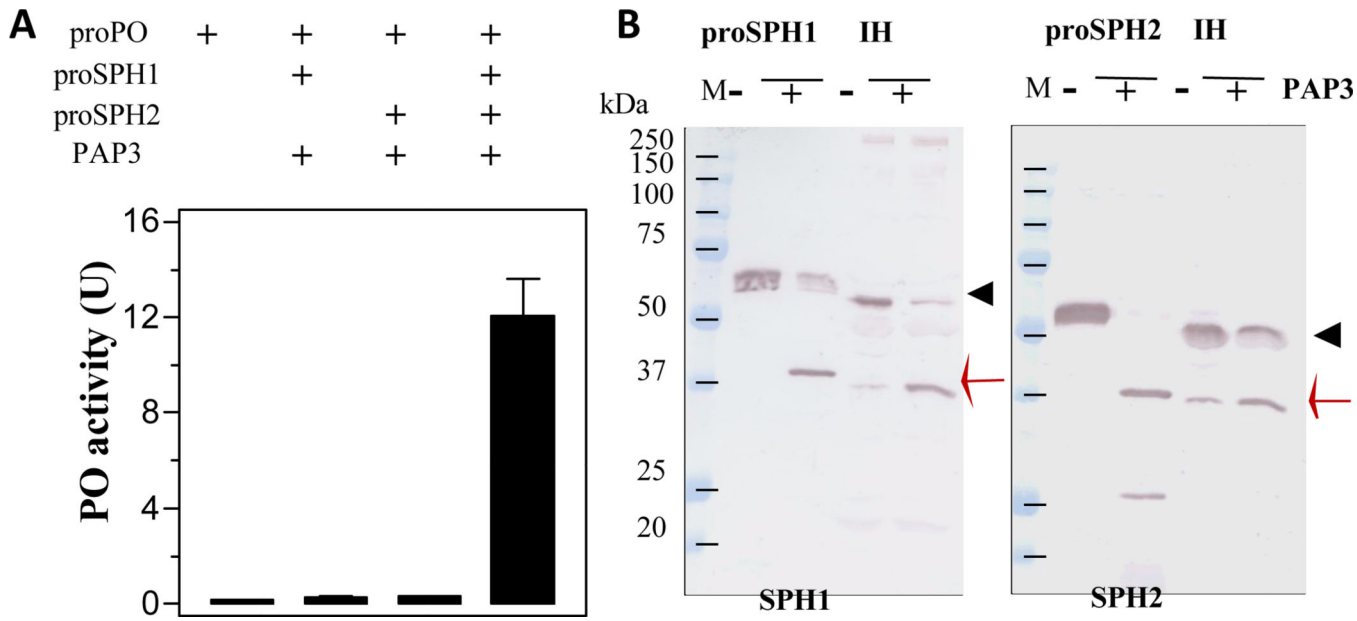

Fig. 5. Cleavage activation of the proSPHs and proPOs by PAP3

As described in *Section 2.4*, buffer (20 mM Tris-HCl, pH 7.5, 0.5 μl), proSPH1 (50 ng, 0.5 μl), proSPH2 (50 ng, 0.5 μl), and both proSPHs (50 ng each, 1 μl total) were separately reacted with purified PAP3 (20 ng, 1 μl), proPOs (400 ng, 1 μl), and the buffer (46.5 μl) for 1 h on ice, PO activities were measured and plotted as mean ± SEM (n = 3) (panel A). To detect cleavage of the proSPHs and compare their product sizes with those generated in plasma, the purified recombinant proSPH1 or proSPH2 (100 ng, 1 μl) was incubated on ice for 1 h with PAP3 (20 ng, 1 μl) and 20 mM Tris-HCl, pH 7.5 (10 μl). Induced hemolymph (IH, 2 μl), PAP3 (20 ng, 1 μl), 0.1% PTU (1 μl), and 20 mM Tris-HCl, pH 7.5 (11 μl) were incubated at room temperature for 15 min. In the control reactions, PAP3 was replaced by equal volume of the buffer. After treatment with SDS sample buffer, all the reaction mixtures were separated by 10% SDS-PAGE, electrotransferred onto nitrocellulose membrane, and detected using 1:2,000 diluted SPH1 or SPH2 antiserum as the first antibody (panel B). Positions of the proSPHs (*black triangle*) and their cleavage products (*red arrow*) are marked. Sizes and positions of the marker proteins are indicated.

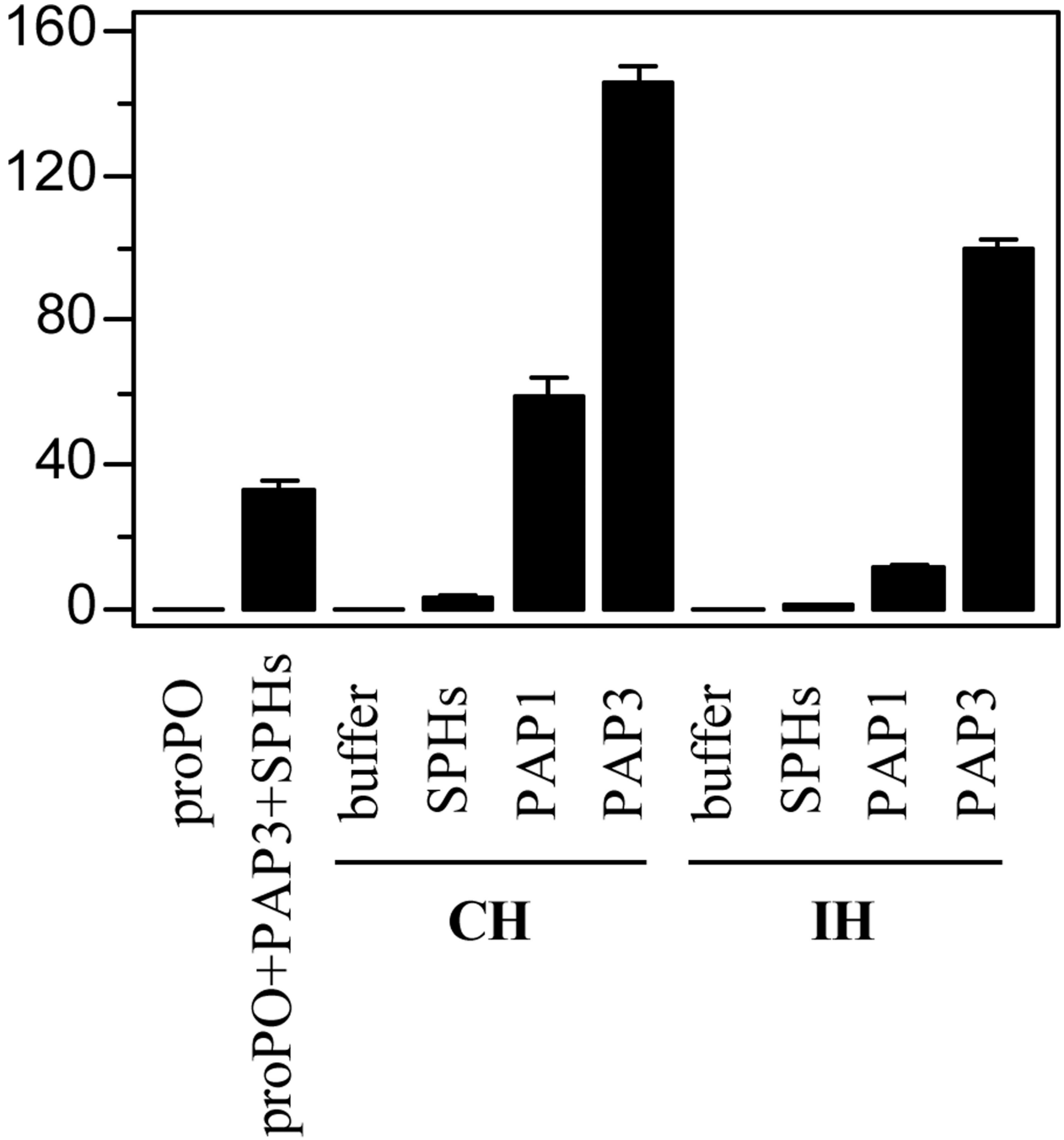

Fig. 6. PAP3-mediated large enhancement of proPO activation in control (CH) and induced (IH) hemolymph from *M. sexta* larvae

As described in *Section 2.6*, the cell-free hemolymph samples (1 μl, CH or IH) from naive or bacteria-injected larvae and 20 mM Tris-HCl, pH 7.5 (18 μl) were separately incubated with 1 μl of the buffer, purified SPHs (20 ng), PAP1 (20 ng), or PAP3 (20 ng) at room temperature for 15 min. In the control set, proPOs (100 ng, 1 μl) was either incubated with the buffer (19 μl) or buffer (17 μl) with purified SPHs (20 ng, 1 μl) and PAP3 (20 ng, 1 μl) on ice for 1 h. PO activities in the control and test samples were determined and plotted in the bar graph as mean ± SEM (n = 3).

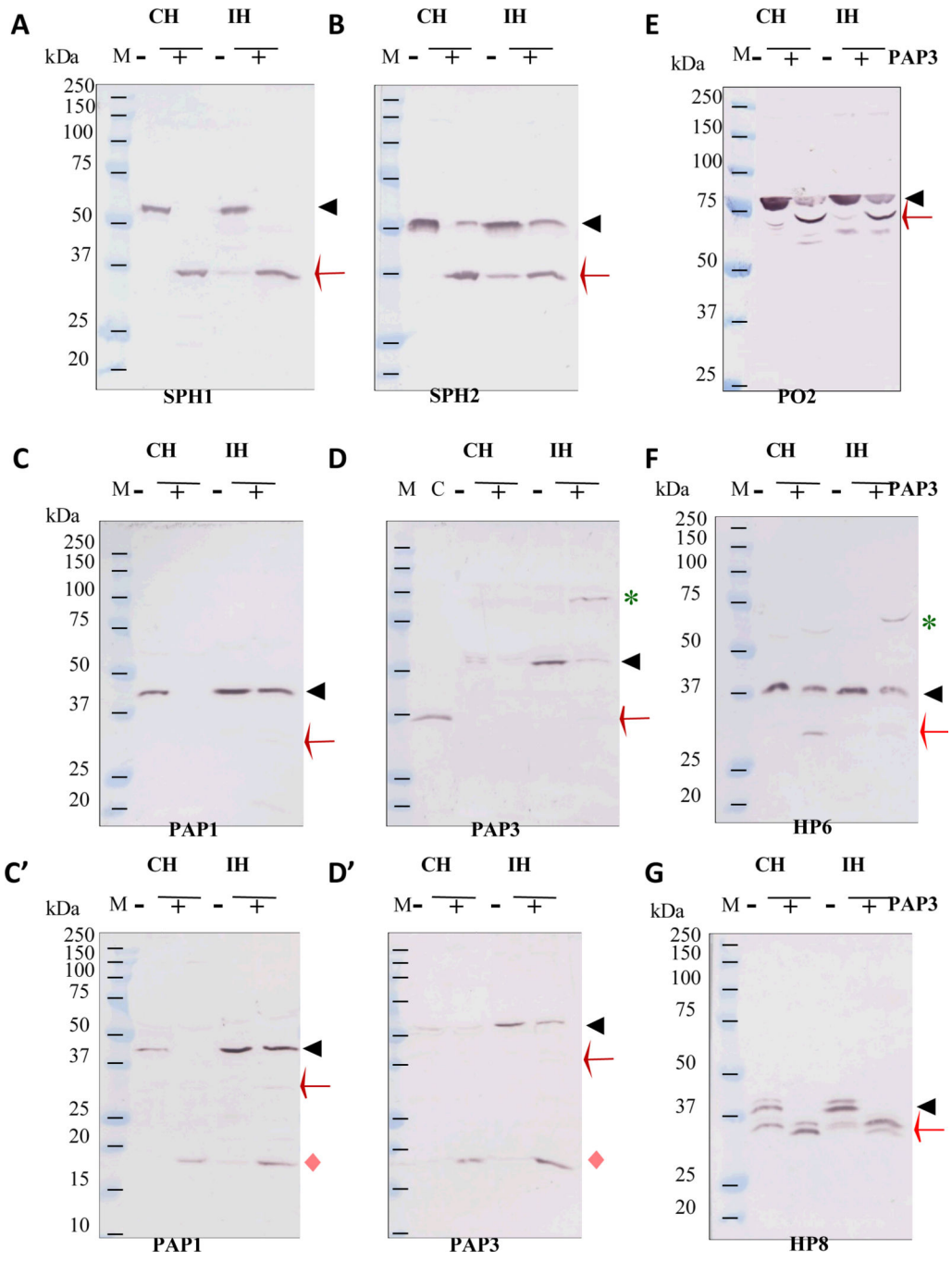

Fig. 7. Proteolytic activation of *M. sexta* HP6, HP8, PAP1, PAP3, SPH1, SPH2, PO2 precursors in CH and IH accompanying the large increase in PO activity triggered by PAP3

As described in *Section 2.7*, the plasma samples (30 μl), 0.1% PTU (15 μl), 20 mM Tris-HCl, pH 7.5, 0.001% Tween-20 (165 μl) were incubated with PAP3 (300 ng, 15 μl) or the buffer (15 μl) at room temperature for 15 min. The reaction mixtures were treated with SDS sample buffer and one-fifteenth of the samples were analyzed by SDS-PAGE (10% for panels A, B, C, D, F, and G; 12% for C' and D'; 7.5% for panel E). Following electrotransfer, the protein blots were separately incubated with 1:2,000 diluted antisera against SPH1 (A), SPH2 (B), PAP1 (C and C'), PAP3 (D and D'), PO2 (E), HP6 (F) and

HP8 (G), as indicated in the bottom of each panel. The antibody-antigen complexes were detected using alkaline phosphatase-conjugated goat-anti-rabbit antibodies. Sizes and positions of the marker proteins (250, 150, 100, 75, 50, 37, 25, 20, 15, and 10 kDa) are shown as short bars, whereas positions of the precursor proteins (*black triangles*), cleavage products (*red arrow* for heavy chain and *pink diamond* for light chain), and putative serine proteinase-serpin complexes (*green asterisk*) are indicated.

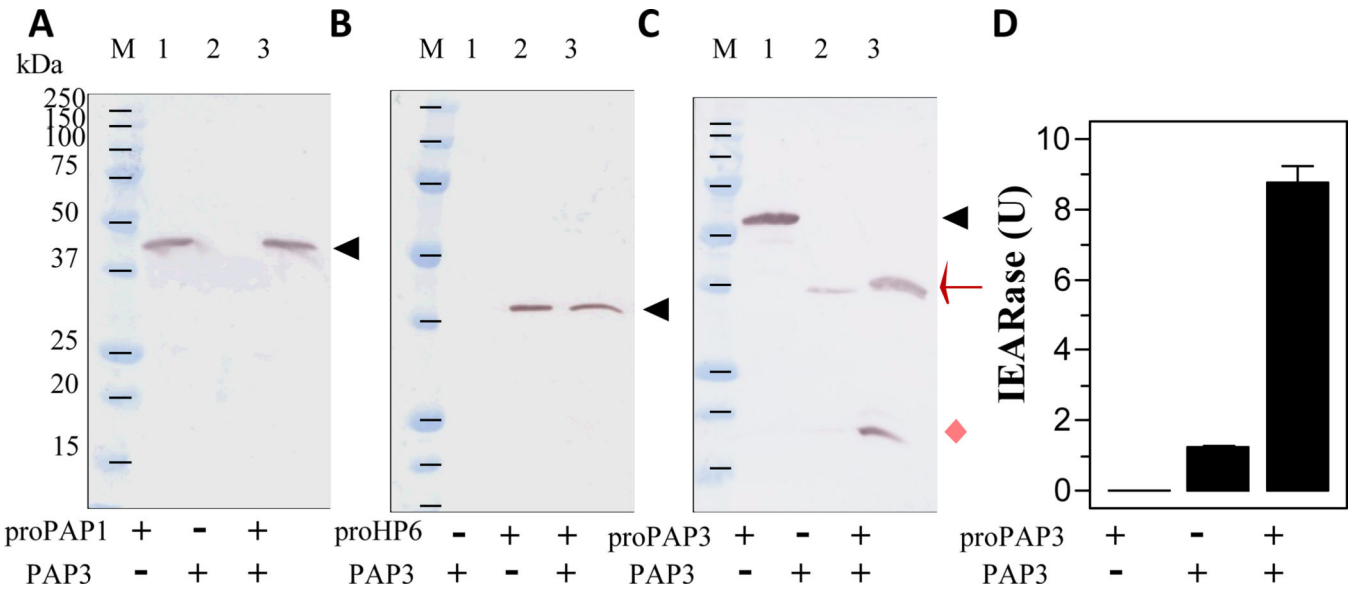

Fig. 8. Examination of possible proPAP1, proHP6, and proPAP3 cleavage by PAP3

As described in *Section 2.8*, the purified recombinant proPAP1 (200 ng, 2 μl), proHP6 (100 ng, 2 μl), and proPAP3 (200 ng μl) were individually incubated with buffer (20 mM Tris-HCl, pH 7.5, 0.001% Tween-20, 12 μl) or PAP3 (40 ng, 2 μl and the buffer, 10 μl) at room temperature for 1 h. The reaction mixtures and PAP3 only (40 ng, 2 μl and the buffer, 12 μl) were subjected to SDS-PAGE (15% for PAP1 and PAP3; 10% for HP6) and immunoblot analysis using PAP1 (panel A), HP6 (panel B), and PAP3 (panel C) antibodies. The positions of zymogens (*black triangle*), catalytic domain (*red arrow*), and PAP3 light chain (*pink diamond*) are indicated. To test if proPAP3 activation by PAP3 results in additional IEAR*p*NA hydrolysis, proPAP3 (200 ng, 2 μl and buffer, 18 μl), PAP3 (40 ng, 2 μl and buffer, 18 μl), and proPAP3 (200 ng, 2 μl), PAP3 (40 ng, 2 μl), and buffer (16 μl) were incubated at room temperature for 1 h. The IEARase activities were measured and plotted in the bar graph as mean ± SEM (n = 3) (panel D).

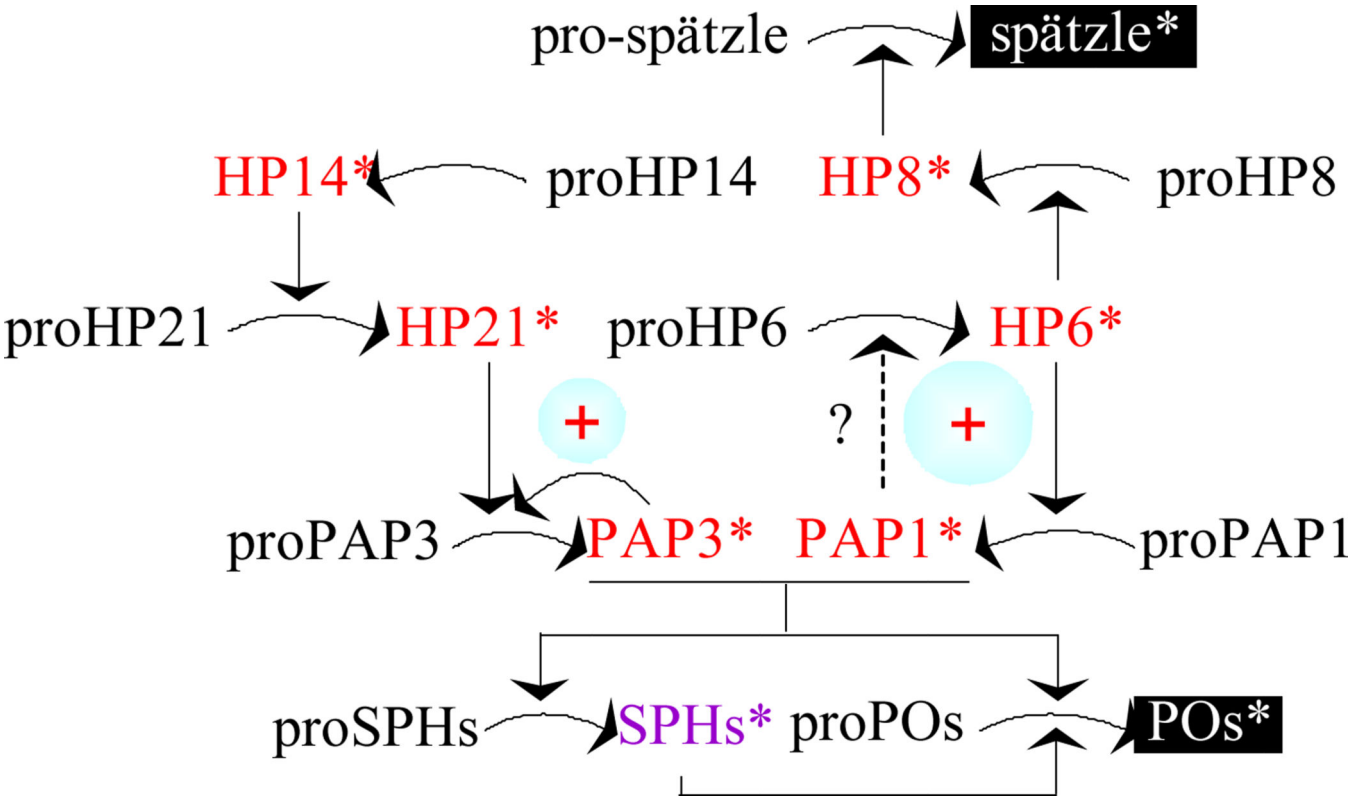

Fig. 9. A model for PAP3-stimulated proPO activation

Based on this study, PAP3 activates proPAP3 to generate more PAP3, which cleaves proSPH1 and proSPH2 to form an SPH complex. In the presence of this complex, PAP3 activates proPOs to form active POs. While PAP3 does not directly activate proPAP1 or proHP6, its addition to CH or IH causes proHP6 activation and HP6 activates proHP8 and proPAP1 to reinforce PO production and melanization (An et al., 2009). The activation of proPAP3 does not seem to involve HP14 or HP21, a direct activator of proPAP2 and proPAP3 (Wang and Jiang, 2007; Gorman et al., 2007). HP8 activates *M. sexta* pro-spätzle to induce synthesis of antimicrobial proteins (An et al., 2010). In comparison, *T. molitor* SPE itself generates SPH, PO, and spätzle (Kan et al., 2008; Roh et al., 2009).